MADRID
inter.noise 2019
June 16 - 19
NOISE CONTROL FOR A BETTER ENVIRONMENT

Dynamic behavior and power flow analysis of Acoustic Black Hole beams

Yuhang Wang [1]
Jingtao Du[1]
College of Power and Energy Engineering,
Harbin Engineering University,
Harbin, 150001, P.R. China

Li Cheng[2]
Department of Mechanical Engineering,
The Hong Kong Polytechnic University,
Hong Kong, 999077, P.R. China

ABSTRACT

A truthful description of the energy transport process, which can be depicted by a physical quantity, namely power flow, is a significant angle to understand the Acoustic Black Hole (ABH) effect and its applications. To tackle the defect of existing semi-analytical models on ABH structures in calculating the higher-order derivatives of structural displacement, an energy formulation, in conjunction with a Rayleigh-Ritz procedure, is proposed for an ABH beam, in which the transverse displacement is constructed using Fourier series with supplementary terms. This treatment ensures the continuity and the smoothness of all relevant derivatives terms in the entire calculation domain, thus allowing the calculation of the power flow and structural intensity. Numerical examples are presented to illustrate the reliability and effectiveness of the established model. Numerical analyses on the dynamic behavior and power flow show the spatial and frequency characteristics of energy transmission process and reveal the ABH working mechanisms. While providing an efficient analysis tool, this work enriches the existing understanding on the dynamic behavior of ABH structures.

Keywords: ABH beam; power flow; structural intensity; Fourier series

1. INTRODUCTION

The Acoustic Black Hole (ABH) phenomenon, featuring a gradual phase velocity reduction of the flexural waves in a thin-walled structure with a power-law tailored decreasing thickness, has been explored for various applications. Thanks to its unique wave retarding and energy focalization feature, significant vibration attenuation can be achieved by using a small amount of damping near the tip of the ABH taper. Since the pioneer work of Mironov [1] and a series of significant work of Krylov *et al.* [2-5], interest in exploring various aspects of ABH has experienced a flourishing development

[1] dujingtao@hrbeu.edu.cn

in the past twenty years. Typical work ranges from theoretical to experimental studies as well as various applications in both ABH beams [6-8] and plane structures of various shapes such as circular [9,10], elliptical [11,12] and rectangular plates [13].

It is very significant to understand the wave propagation process and efforts have been made using different metrics such as reflection coefficient [14], cross-point mobility [8,15,16] and energy distribution [17,18] etc. As a useful attempt, experimental approach was adopted to visualize the wave propagation using a combined laser excitation technique and laser scanning vibrometer measurement [17].

A predictive model capable of characterizing the energy transport process in ABH structure is of great interest to guide the practical design of ABH structures. Apart from the widely used FEM/BEM methods, effort has also been made in developing semi-analytical modeling techniques for beams [8] and plates [19] based on different types of wavelets [8, 15], and these works show the advantages of the semi-analytical modeling and its accuracy in predicting the structural response.

Motivated by this, a revamped semi-analytical modeling approach is proposed in this paper for power flow analysis of an elastically restrained ABH beam. Energy formulation in conjunction with Rayleigh-Ritz procedure is employed for the dynamic description of the ABH beams. Numerical examples are then presented to validate the correctness and effectiveness of the proposed model through the comparison with results from other approaches. Using the proposed model, power flow and structural intensity in ABH beam are studied. Finally, conclusions are given.

2. THEORETICAL FORMULATION

2.1 Elastically Restrained ABH Beam

As illustrated in Figure 1, we consider a Euler-Bernoulli ABH beam undergoing transverse vibration under a concentrated force excitation F at x_f, with the coordinate origin being located at the left end of the beam. The whole system is assumed to be symmetrical with respect to the mid-line. The beam, having a length L and a constant width b, has a variation thickness profile $h(x)$ and is symmetrically covered by a damping layer of thickness h_d.

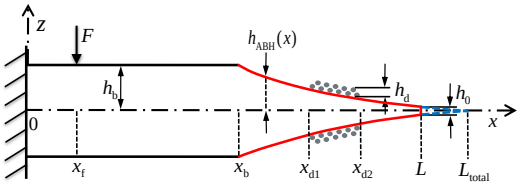

Figure 1 Elastically retrained ABH beam with damping layers fully coupled

The thickness variation function across the entire ABH beam (including a uniform part and ABH part) is expressed as:

$$h(x)=\begin{cases} h_b & ,0\le x\le x_b \\ \varepsilon(L_{total}-x)^m & ,x_b<x\le L \end{cases} \tag{1}$$

As shown in Figure 1, other geometrical parameters, such as the total length L_{total} and the inevitable thickness truncation results from the practical manufacturing limitation, h_0. Boundary conditions of the beam are simulated by introducing a set of elastic springs at both ends against translation and rotation, respectively. Through a proper assignment of the restraining spring coefficients, all the classical boundary conditions as well as their combinations can be readily simulated. Structural damping is simulated through a complex Young's modulus $E=E(1+j\eta)$, with η being the damping loss factor, taking different values for the beam and the damping layer.

2.2 Fully Coupled Dynamic Modelling of ABH Beam

A fully coupled dynamic model is established based on the Euler-Bernoulli beam theory and energy principle. The system Lagrangian L_s can be written as

$$L_s = V - T - W \tag{2}$$

where V and T are the total potential and kinetic energies, including the elastic boundary restraints as well as the damping layers. W is the work done by the concentrated force applied at the beam structure.

The potential energy V writes:

$$\begin{aligned} V = \frac{1}{2}\left(\int_0^L E_b I_b(x) \left(\frac{\partial^2 w(x)}{\partial x^2} \right)^2 \mathrm{d}x + \int_{x_{d1}}^{x_{d2}} E_d I_d(x) \left(\frac{\partial^2 w(x)}{\partial x^2} \right)^2 \mathrm{d}x \right) \\ + \frac{1}{2} K_b \left(\frac{\partial w(x)}{\partial x} \right)_{x=0}^2 + \frac{1}{2} k_b \left(w(x) \right)_{x=0}^2 \end{aligned} \tag{3}$$

in which, the two terms in the first row are related to the strain potential energies due to the traverse deformation of the host ABH beam and the damping layers, respectively. Here, damping layers cover the beam surface region [x_{d1}, x_{d2}]. The remaining two terms in the second row represent the elastic potential energies stored in the rotational and translational springs at clamped end.

The kinetic energy T can be written as:

$$T = \frac{1}{2}\omega^2 \left(\rho_b \int_0^L S_b(x) w(x)^2 \mathrm{d}x + \rho_d \int_{x_{d1}}^{x_{d2}} S_d(x) w(x)^2 \mathrm{d}x \right) \tag{4}$$

In the energy expressions above, the material parameters are distinguished by superscripts, respectively. And the work W done by the external point force excitation is:

$$W = \int_0^L F \delta(x - x_f) w(x_f) \mathrm{d}x \tag{5}$$

where F denotes the external force and $\delta(x)$ is the Dirac delta function to define the excitation position at x_f.

2.3 Improved Fourier Series Solution

With the aim to satisfy the differential continuity requirements by the force equilibrium and geometric coordination at the general elastic end supports, the standard Fourier series is supplemented by boundary smoothened auxiliary functions as follows:

$$w(x) = \sum_{m=0}^{\infty} C_m \cos(\lambda_{Lm} x) + \sum_{i=1}^{4} c_i \zeta_i(x) \tag{6}$$

in which $\zeta_i(x)$ are four auxiliary functions, weighted by four coefficients c_i (i=1,2,3 and 4). In conjunction with Rayleigh-Ritz procedure, the discretized system equation can be derived and expressed in the following matrix form

$$(\mathbf{K} - \omega^2 \mathbf{M})\mathbf{R} = \mathbf{F} \tag{7}$$

where **M** and **K** are the mass and stiffness matrices, respectively; ω is the angular frequency; **R** and **F** are the coefficient vectors of the improved Fourier series expansion and the external force loading, respectively. Equation 7 can be solved through standard matrix inversion operation. By removing the force vector on the right-hand side, all the modal information can be obtained by solving a standard eigen-value problem. Substitution of the corresponding eigenvector into the improved Fourier series displacement expression, one can get the mode shapes of the ABH beam structure.

2.4 Power Flow and Structural Intensity of ABH Beam

Thanks to the satisfactory derivative continuity characteristics of the constructed ABH beam flexural displacement expression, all the internal force required in the structural intensity analysis can be determined in a much straightforward pattern through term-by-term differential operation. The input time-averaged power flow Pinput is defined as:

$$P_{\text{input}} = \frac{1}{T_{\text{P}}} \text{Re}\left\{ \int_0^{T_{\text{P}}} F(t) v(t) \text{d}t \right\} \tag{8}$$

where $v(t)$ is the vibrational velocity at the force application position; t and T_{p} are the time and observation period, respectively.

As to the vibration energy transmission in the beam structure, the structural intensity $I_{x,\text{transfer}}$， which is defined as a vibration power flow through per unit cross sectional area of the beam, is expressed as:

$$I_{x,\text{transfer}}(x) = \frac{1}{2} \text{Re}\left\{ Q_x \left(\frac{\partial w}{\partial x} \right)^* - M_x \left(\frac{\partial^2 w}{\partial x \partial t} \right)^* \right\} \tag{9}$$

3. NUMERICAL RESULTS AND DISCUSSIONS

3.1 Model Validation

To check and demonstrate the ability of current model for ABH beam structure. The forced vibration is analyzed for this ABH beam structure, with a unit point force. Presented in Figure 2 is a comparison of the acceleration response of the ABH beam, calculated from the current model and FEM, respectively. Two representative mode shapes, namely the fifth and twentieth modes, are also given in the figure. From this figure, it can be observed that both the trend and magnitude of vibration frequency response, as well as the two arbitrarily selected mode shapes, agree very well with each other between these two approaches in the whole frequency range of interest. Various resonant peaks in the frequency response curve actually correspond to the structural modes of the ABH beam.

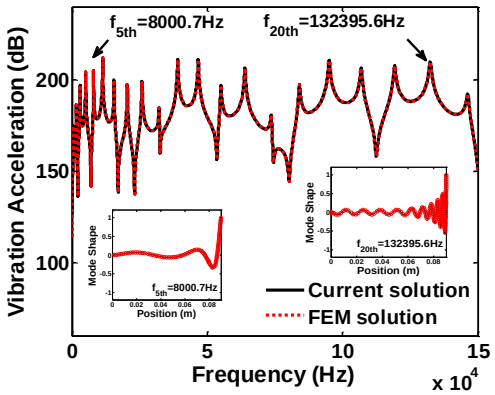

Figure 2 Comparison of vibration acceleration response of ABH beam calculated from the current model and FEM in COMSOL

3.2 Power Flow and Structural Intensity of ABH Beam Without Damping Layers

The total input power can be estimated from the applied force amplitude and point mobility. Two representative observing points are also chosen for the computation of transfer power flow, for which oneis located in the uniform region of the beam, whilst the other in the ABH region. Figure 3 presents the variation of the total input power and power flow at the two observing points.

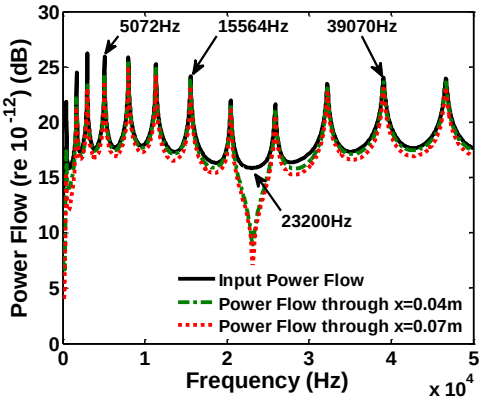

Figure 3 Frequency response of the total input and transfer power flow in ABH beam structure

The power flow can be estimated from the applied force amplitude and point mobility. In order to better understand the energy transport process and its underlying mechanism associated with the ABH beam, structural intensity distribution across the entire beam is examined for some representative modal frequencies, namely f_4=5072Hz and f_{11}=39070Hz, as shown in Figure 4. In the subplots, the positive and negative values of structural intensity denote the power flow to the right and left direction across each field point, respectively. In Figure 4(a), the excitation position clearly separates two different zones with positive and negative structural intensity distribution, indicating two opposite energy flow directions. With the increase of frequency, at 39070Hz, a relatively uniform gradient of structural intensity distribution can be observed Figure 4(b).

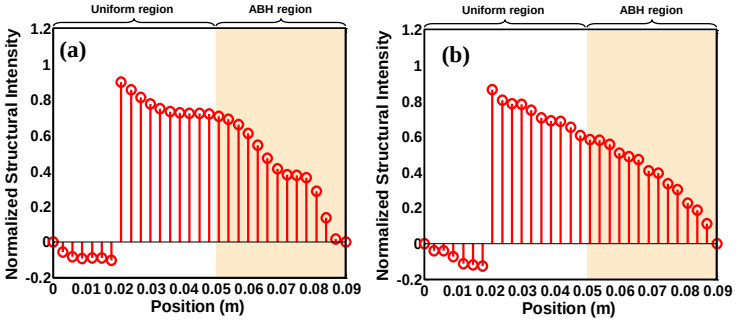

Figure 4 Normalized structural intensity distribution in ABH beam under resonant excitation frequencies: (a) 5072Hz; (b) 39070Hz

3.2 Energy Transmission in ABH Beam with Damping Layers

In principle, complete ABH effect takes place only with the use of the damping layers due to the existence of the truncated thickness at the taper. With this in mind, the same beam as the one used above but with additional damping layers is investigated. Damping layers are bonded over part of the ABH region at the tip.

Presented in Figure 5 is the structural intensity distribution of the ABH beam with damping layers, with results denoted by a black square. For the comparison purpose, the results of the ABH beam without damping layers shown in Figure 6 are also given here again, marked as a red circle. For convenience, different regions of the beams are marked as shadowed areas of different colors. Generally speaking, a relatively flat structural intensity distribution is observed within the uniform portion of the beam. The trend persists until the entrance of the coating area, starting from which a sudden and rapid decrease is produced. At the 5072 Hz, fluctuations associated with the structural intensity variation can be observed. When frequency

increases, the overall trends will become more uniform and smoother.

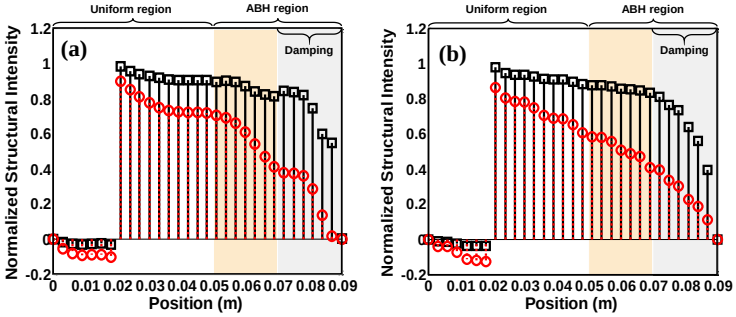

Figure 5 Damping layers effect on the normalized structural intensity distributions of ABH beam under excitation frequencies: (a) 5072Hz; (b) 39070Hz

4. CONCLUSIONS

In this paper, a novel semi-analytical model for power flow and structural intensity analysis of an elastically restrained Euler-Bernoulli ABH beam is established. An energy formulation is employed for the dynamic description of ABH beams. Under Rayleigh-Ritz framework the problem can be solved.

Numerical examples are presented to validate the proposed model. With the model established, power flow and structural intensity analyses of ABH beam without and with damping layers are carried out. It can be seen that for the bare ABH beam without damping layer,with the frequency increasing, the gradient of the structural intensity distribution becomes more uniform and a global increase in the normalized structure intensity is observed as compared with its counterpart without damping layers with the damping layers covering the tip part of the ABH beam.

This work establishes a semi-analytical model for the power flow analysis of elastically restrained ABH beam for the first time, which can be used for energy transmission mechanism study and further optimal design of ABH beam structure.

5. ACKNOWLEDGEMENTS

This work was supported by the Fok Ying Tung Education Foundation (Grant no. 161049). The authors would also like to thank the financial support from the Research Grant Council of the Hong Kong SAR (PolyU 152009/15E and PolyU 152026/14E), National Science Foundation of China (No. 11532006).

6. REFERENCES

[1] M.A. Mironov, *"Propagation of A Flexure Wave in A Plate Whose Thickness Decreases Smoothly to Zero in A Finite Interval"*, Soviet Physics Acoustics (1988)

[2] V.V. Krylov, *"Conditions for Validity of the Geometrical-Acoustics Approximation in Application to Waves in an Acute-Angle Solid Wedge"*, Soviet Physics Acoustics (1989)

[3] V.V. Krylov, *"Geometrical-Acoustics Approach to The Description of Localized Vibrational Modes of an Elastic Solid Wedge"*, American institute of physics (1990)

[4] V.V. Krylov, *"Localized Acoustic Modes of a Quadratically-Shaped Solid edge"*, Moscow University Physics Bulletin (1990)

[5] V.V. Krylov, *"Propagation of Localized Vibration Modes Along Edges of Immersed Wedge-Like Structures: Geometrical-Acoustics Approach"*, Journal of Computational Acoustics (1999)

[6] V.V. Krylov, F.J.B.S. Tilman, *"Acoustic 'black holes' for flexural waves as effective vibration dampers"*, Journal of Sound and Vibration (2004)

[7] V.V. Krylov, *"New Type of Vibration Dampers Utilising the Effect of Acoustic 'Black Holes'"*, Acta Acustica United with Acustica (2004)

[8] L.L. Tang, L. Cheng, H.L. Ji, J.H. Qiu, *"Characterization of Acoustic Black Hole Effect Using a One-Dimensional Fully-Coupled and Wavelet-Decomposed Semi-Analytical Model"*, Journal of Sound and Vibration (2016)
[9] D.J. O'Boy, V.V. Krylov, *"Damping of Flexural Vibrations in Circular Plates with Tapered Central Holes"*, Journal of Sound and Vibration (2011)
[10] D.J. O'Boy, E.P. Bowyer, V.V. Krylov, *"Point Mobility of a Cylindrical Plate Incorporating a Tapered Hole of Power-Law Profile"*, Acoustical Society of America Journal (2011)
[11] V.B. Georgiev, J. Cuenca, M.A.M. Bermudez, F. Gautier, L. Simon, *"Recent Progress in Vibration Reduction Using Acoustic Black Hole Effect"*, 10ème Congrès Français d'Acoustique, Lyon (2010)
[12] V.B. Georgiev, J. Cuenca, F. Gautier, L. Simon, V.V. Krylov, *"Damping of Structural Vibrations in Beams and Elliptical Plates Using the Acoustic Black Hole Effect"*, Journal of Sound and Vibration (2011)
[13] E.P. Bowyer, D.J. O'Boy, V.V. Krylov, *"Damping of Flexural Vibrations in Plates Containing Ensembles of Tapered Indentations of Power-Law Profile"*, 164th Meeting of the Acoustical Society of America, Kansas (2012)
[14] V. Denis, F. Gautier, A. Pelat, J. Poittevin, *"Measurement And Modelling Of The Reflection Coefficient Of An Acoustic Black Hole Termination"*, Journal of Sound and Vibration (2015)
[15] L.L. Tang, L. Cheng, *"Enhanced Acoustic Black Hole Effect in Beams with A Modified Thickness Profile and Extended Platform"*, Journal of Sound and Vibration (2017)
[16] S.C. Conlon, P.A. Feurtado, *"Progressive Phase Trends in Plates with Embedded Acoustic Black Holes"*, Journal of the Acoustical Society of America (2018)
[17] H.L. Ji, J. Luo, J.H. Qiu, L. Cheng, *"Investigations On Flexural Wave Propagation and Attenuation in A Modified One-Dimensional Acoustic Black Hole Using a Laser Excitation Technique"*, Mechanical Systems and Signal Processing (2018)
[18] Huang W, Ji H, Qiu J, et al, *"Analysis of Ray Trajectories of Flexural Waves Propagating Over Generalized Acoustic Black Hole Indentations"*, Journal of Sound and Vibration (2018)
[19] L. Ma, S. Zhang, L. Cheng, *"A 2D Daubechies Wavelet Model On the Vibration of Rectangular Plates Containing Strip Indentations with A Parabolic Thickness Profile"*, Journal of Sound and Vibration (2018)